

Sensitivity studies for searches for electroweak supersymmetry during run-II of the LHC

by

Sesegma Sanzhieva

A thesis submitted in fulfilment
of the requirements for the degree of
Bachelor of Science
in Maastricht University

TABLE OF CONTENTS

ABSTRACT	iii
CHAPTERS	
I. Introduction	1
II. Background information (provisional title)	3
2.1 The Standard Model	3
2.1.1 The overview of the Standard Model	3
2.1.2 Limitations of the SM	4
2.2 Supersymmetry	6
2.3 The ATLAS detector	7
2.3.1 The ATLAS sub-detectors and trigger systems . . .	8
III. Search for supersymmetry at the LHC	11
3.1 Introduction	11
3.2 General search methods	14
3.3 Overview of background processes	16
3.4 Event selection and b -tagging	16
3.4.1 Event variables used in the analysis	17
3.5 Cut-and-count approach and test statistics	18

ABSTRACT

CHAPTER I

Introduction

High Energy Physics (HEP) is a branch of physics that studies elementary particles. The main way of studying physics experimentally at subatomic level is using particle accelerators. Specific particles are accelerated to high speeds and directed to collide with each other producing an array of other particles that are then registered by detectors and studied by physicists. The largest currently functioning HEP experiment is the Large Hadron Collider (LHC) at CERN in Geneva, Switzerland. Since 2015 it is able to accelerate protons and creates collisions at a centre-of-mass energy of 13 TeV. These collisions happen at two sites where main particle detectors are situated. These experiments are ATLAS (A Toroidal LHC Apparatus) and CMS (Compact Muon Solenoid). Such high energy conditions of collisions emulate the state of the universe very shortly after the Big Bang and thus allow creation of particles that don't exist at normal conditions.

The underlying theory of modern HEP is the Standard Model and it has been very successful in describing subatomic particles and the interactions between them. It is a very robust theory that has been tested through a plethora of experiments at colliders. The most prominent success of previous LHC runs at 7 and 8 TeV centre-of-mass energy was the discovery of the Higgs particle, which was the final SM particle whose existence was proven experimentally [1, 2].

However, there are limitations to SM and there are a number of theories that try address these shortcomings. Collectively they are known as Beyond-the-Standard-Model (BSM) theories and present new theoretical frameworks aiming to explain physical world at a deeper level. One of the major BSM theories is Supersymmetry. It has a mathematically effective and elegant representation and, most importantly, overcomes some critical SM limitations.

Searches for evidence of supersymmetry are performed at the LHC along with other particle experiments. After runs at 7 and 8 TeV no significant evidence was

found and limits on masses of hypothetical supersymmetric particles have been placed. Higher energy collisions present a better chance of finding evidence of supersymmetry. The research presented in this thesis focuses on trying to design search methods in run-II (13 TeV) data that are sensitive to particular SUSY scenarios that feature electroweak production and decay. For that purpose a set of kinematic and topological variables are investigated as ways to determine presence of new particles.

CHAPTER II

Background information (provisional title)

2.1 The Standard Model

2.1.1 The overview of the Standard Model

The underlying theory of modern High Energy Physics is the Standard Model (SM). This theory has been developed in the second half of the 20th century with contributions from many scientists and it is a very successful representation of the world on subatomic level. The SM classifies all known subatomic particles into specific categories and provides the description of the interactions between them.

In SM there are two main types of fermions (1/2-spin particles) known as quarks and leptons. Each family has three generations with each consecutive generation being heavier than the previous. The up and down quarks along with the electron are stable and constitute ordinary matter. The interactions between fermions are mediated through the exchange of force carrier particles known as gauge bosons (see Tab. 2.1). The final piece in SM is the Higgs boson and it gives mass to other fundamental particles. All bosons possess integer spin [3]. Further nomenclature identifies hadrons - composite particles that are made of quarks and gluons.

The mathematical representation of SM is built within the broader frame of Group Theory. Employing the official terminology, SM has the symmetry group

Fermion	Generations			Bosons
Leptons	e	μ	τ	Z
	ν_e	ν_μ	ν_τ	W^\pm
Quarks	u	c	t	photon
	d	s	b	gluon

Table 2.1: The Standard Model particles

$U(1)_Y \times SU(2)_L \times SU(3)$. The $SU(3)$ symmetry group generates strong interactions, that describe processes involving quarks and gluons. These processes are described by the theory of Quantum Chromodynamics and the particles possess a specific type of charge known as "colour charge". The $U(1)_Y \times SU(2)_L$ generates electroweak interactions. At the energies below 100 GeV, however, the single electroweak interaction is broken into the weak and electromagnetic varieties with the symmetry group $U(1)_{em}$. The unification of these two types was the result of efforts by Glashow, Weinberg and Salam [4, 5, 6]. The weak interaction processes involve fermions and are mediated by electrically charged W^\pm for charged processes and chargeless Z gauge boson for neutral ones. Electromagnetic force is mediated by photons and only involves electrically charged particles.

Above the unification energy of 100 GeV, and thus before the spontaneous electroweak symmetry breaking through Higgs mechanism [7, 8], the gauge bosons are different. There are three W bosons, denoted W^1, W^2, W^3 corresponding to $SU(2)_L$ part of the group and one B boson corresponding to $U(1)_Y$. All the electroweak bosons are massless, and acquire mass by coupling to the Higgs field in the process of symmetry breaking.

2.1.2 Limitations of the SM

The predictions of the SM have been successfully tested in particle accelerator experiments, and the final confirmation came with the discovery of the Higgs boson in 2012 - a true scientific breakthrough. This was the last missing piece of experimental evidence needed for the full validation of SM. The experiments that led to this discovery were conducted at CERNs Large Hadron Collider (LHC) in run-I proton-proton collisions at centre-of-mass energy $\sqrt{s} = 7$ and the later upgrade to 8 TeV. Despite the fact that SM has proven to be an extremely precise and successful theory there are some caveats for which it does not provide adequate solutions.

One of the inconsistencies within SM is the so-called Hierarchy problem [9]. One of the ways it reveals itself is through the large discrepancy between the Planck mass and the mass of the Higgs particle. The former is about 10^{17} times bigger than the latter and current representation of particle physics cannot explain such a big difference. Quantum effects start manifesting themselves at the Plank mass threshold and such a vast difference between these two values is yet unaccounted for.

Another prominent problem is that SM does not explain dark matter. While ordinary matter only constitutes about 5% in the total mass-energy content of the universe, it is dark matter and dark energy that account for the rest [10]. SM does

not provide a candidate particle for dark matter and thus is only able to describe ordinary matter and energy.

One of the main challenges of modern physics is the unification of forces. This is part of the ongoing attempts to reach the ultimate goal - a "theory of everything". Such a theory would have to account for all physical aspects of the universe and include the most fundamental structures and interactions. The first step was made with the unification of electromagnetic and weak forces. The next step is to achieve the unification of electromagnetic, weak, and strong interaction forces this step is called the Grand Unification. The ultimate step is to combine all four fundamental forces together, which means adding gravity, in what is called Super Unification (see Fig. 2.1). Thus far quantum field theory and general relativity are able to describe phenomena on their respective scale of action with remarkable precision, but are fundamentally incompatible.

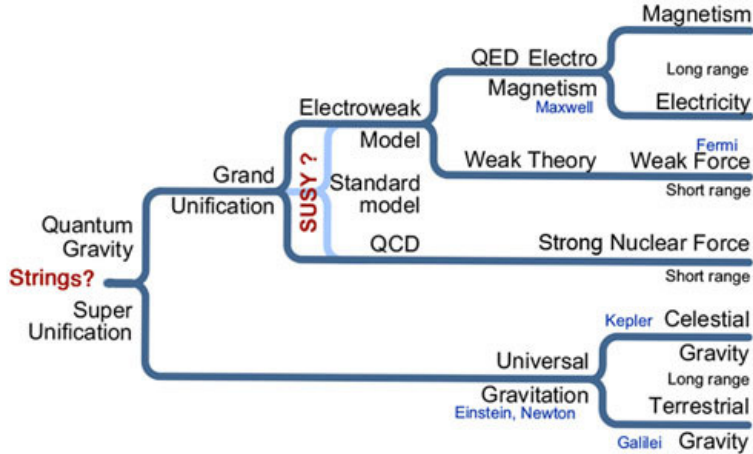


Figure 2.1: Various stages in the unification of forces [11]

Within the confines of the Standard Model even the Grand Unification is not possible, and this prompts the search for new theories that account for this and other shortcomings of SM. Collectively they are called Beyond-Standard-Model (BSM) theories. Among these there are theories that include extra-dimensions, composite Higgs boson models, etc. Theoretical and experimental search for BSM physics is the current frontier in high energy physics and one of the most important questions in science overall.

name	spin	particles
squarks	0	$\tilde{d}_L, \tilde{u}_L, \tilde{s}_L, \tilde{c}_L, \tilde{b}_1, \tilde{t}_1, \tilde{d}_R, \tilde{u}_R, \tilde{s}_R, \tilde{c}_R, \tilde{b}_2, \tilde{t}_2$
sleptons	0	$\tilde{e}_L, \tilde{\nu}_{eL}, \tilde{\mu}_L, \tilde{\nu}_{\mu L}, \tilde{\tau}_1, \tilde{\nu}_{\tau L}, \tilde{e}_R, \tilde{\mu}_R, \tilde{\tau}_2$
charginos	1/2	$\tilde{\chi}_1^\pm, \tilde{\chi}_2^\pm$
neutralinos	1/2	$\tilde{\chi}_1^0, \tilde{\chi}_2^0, \tilde{\chi}_3^0, \tilde{\chi}_4^0$
gluino	1/2	\tilde{g}
Higgs	0	h^0, H^0, A^0, H^\pm

Table 2.2: SUSY particles in MSSM where subscript R denotes right-handed particles and L - left-handed ones. H^0 Higgs boson also exists in SM.

2.2 Supersymmetry

One of the strongest candidate framework theories that can offer solutions to SM deficiencies is Supersymmetry (SUSY) [12]. SUSY is a spacetime symmetry that equates fermionic and bosonic degrees of freedom. Among several theories that are based on SUSY principles, the Minimal Supersymmetric Standard Model (MSSM) offers the simplest extention of SM. MSSM postulates that each SM particle has a supersymmetric partner which is different only in spin by one-half unit (see Table 2.2), while all other quantum numbers stay the same. The superpartners of quarks,

leptons, and neutrinos are called squarks, sleptons and sneutrinos. For gauge bosons the superpartners are gluinos, photino, winos and binos, collectively named gauginos. The latter two are superpartners of the B and three W bosons of the elecrownreak interaction before electroweak symmetry breaking. It follows naturally since SUSY is invoked before the electroweak symmetry breaking. The Higgs sector in SUSY has five superpartners - two charged (H^\pm) sparticles and three neutral ones (h^0, H^0, A^0). They are known collectively as Higgsinos. Mixing between winos, binos and Higgsinos results in charginos and neutralinos. Their mass eigenstates are referred to as $\tilde{\chi}_i^\pm$ ($i = 1,2$) and $\tilde{\chi}_i^0$ ($i = 1,2,3,4$) in order fo increasing mass.

MSSM belongs to a class of theories that all share the same requirement - a quantity known as R-parity has to be conserved in interactions. The mathematical description of R-parity is beyond the scope of this paper. However, one important consequence of R-parity conservation is that if supersymmetric particles were to be produced in collisions, they will be created in pairs. Then they decay through various

possible scenarios with the lightest supersymmetric particle (LSP) emerging in the final state and escaping undetected. Because the LSP is stable it provides a possible candidate for the dark matter particle.

The MSSM imposes 105 free parameters and this is one of its major issues, since any analysis will be addled with enormous complexity stemming from high dimensionality. There are various simplified models that reduce the number of free parameters to manageable values through various theoretically and experimentally motivated constraints. One them is the phenomenological Minimal Supersymmetric Standard Model (pMSSM) that contains only 19 free parameters and it will be used in this thesis' analysis.

2.3 The ATLAS detector

The ATLAS experiment is a multi-purpose particle detector with cylindrical geometry and has a nominal forward-backward symmetry [13]. The dimensions of the detector are 25 m in height and 44 m in length and the overall weight of the detector is approximately 7000 tonnes. It can detect particles with almost 4π coverage in solid angle around the collision point, which covers almost all of the spherical area around the center.

Proton bunches are accelerated in the underground ring that is 27 km in diameter and are directed to collide inside the detectors. The collisions happen at 40 MHz bunch crossing rate, with an average 23 interactions per bunch crossing. The LHC is designed to operate at $\sqrt{s}=14$ TeV and instantaneous luminosity $\mathcal{L} = 10^{34}$ cm $^{-2}$ s $^{-1}$ in proton-proton collision mode. Instantaneous luminosity is defined as follows

$$\mathcal{L} = \frac{1}{\sigma} \frac{dN}{dt} \quad (2.1)$$

Where σ is the interaction cross-section, and N is the number of detected events during time t . Integrated luminosity $\int \mathcal{L} dt$ is a quantity that expresses the amount of total data gathered during the time t of running the LHC. Luminosity is particularly useful as a way to express the amount of data gathered, because it allows to find number of events for a particular process simply by multiplying this process's cross-section by the value of luminosity. The analysis presented in this paper uses the dataset recorded at 3.2 fb $^{-1}$ of integrated luminosity throughout run-II of the LHC during 2015.

The Cartesian coordinate system used at ATLAS has its origin at the nominal

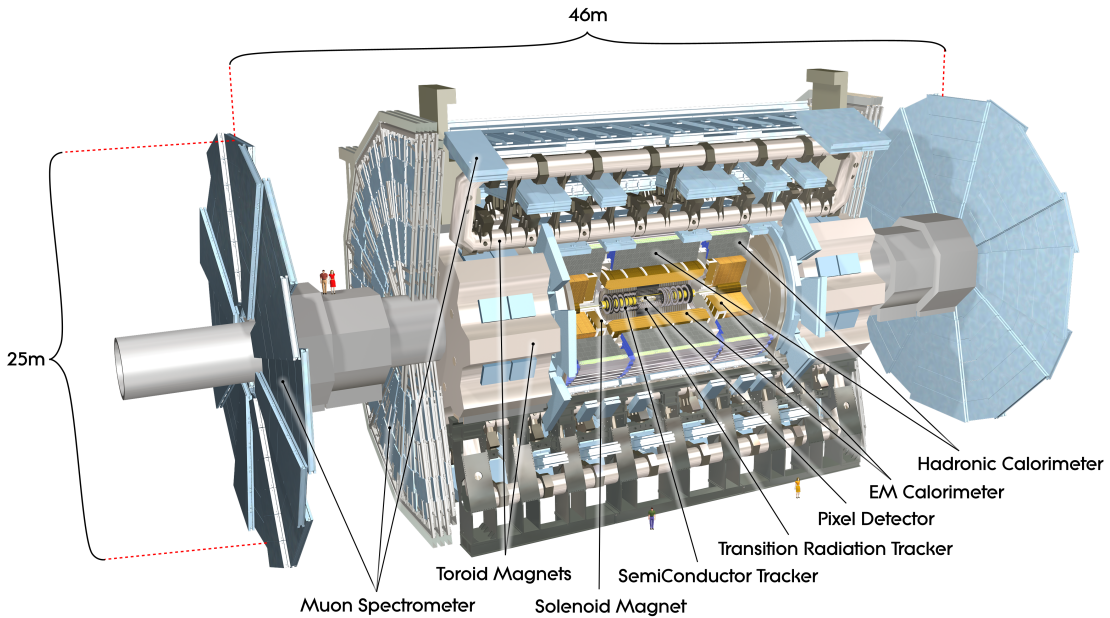


Figure 2.2: Cut-away view of the ATLAS detector (people are included for scale comparison) [13].

point of interaction with z axis extending along the particle beam longitudinally, positive x axis pointing towards the center of the ring, and positive y axis pointing upwards. The geometry of the detector makes the use of cylindrical coordinate system especially convenient. In it, z axis stays the same, the polar angle θ is the angle from z -axis, and the azimuthal angle ϕ encircles z axis in the transverse plane. However, instead of θ it is more convenient to use pseudorapidity η , due to the fact that differences in pseudorapidity are close to invariant under Lorentz boosts along the z axis (fully invariant for real rapidity). η is defined as follows

$$\eta = -\ln\left(\tan \frac{\theta}{2}\right) \quad (2.2)$$

2.3.1 The ATLAS sub-detectors and trigger systems

The ATLAS detector consists of several subdetector layers with each layer performing a specific function (see Fig. 2.3). The Inner Detector (ID) performs tracking of newly created particles. It is closest to the collision point and covers $|\eta| < 2.5$ in pseudorapidity. The ID has high granularity as it is exposed to the highest density of particle interaction. It was designed to provide a transverse momentum resolution

and a transverse impact parameter resolution [14]. The detector itself consists of three separate subsystems. The main components of the ID are: silicon pixel detector, semiconductor tracker, and transition radiation tracker. Ahead of the run-II a new pixel layer, called the Insertable B-Layer (IBL), has been added to the ID improving the resolution and particle identification qualities. All these layers are immersed in a 2 T magnetic field, created by the thin superconducting solenoidal magnet. This field is parallel to the beam axis and bends trajectories of charged particles allowing their charge and momentum identification based on the characteristic bending of their trajectories.

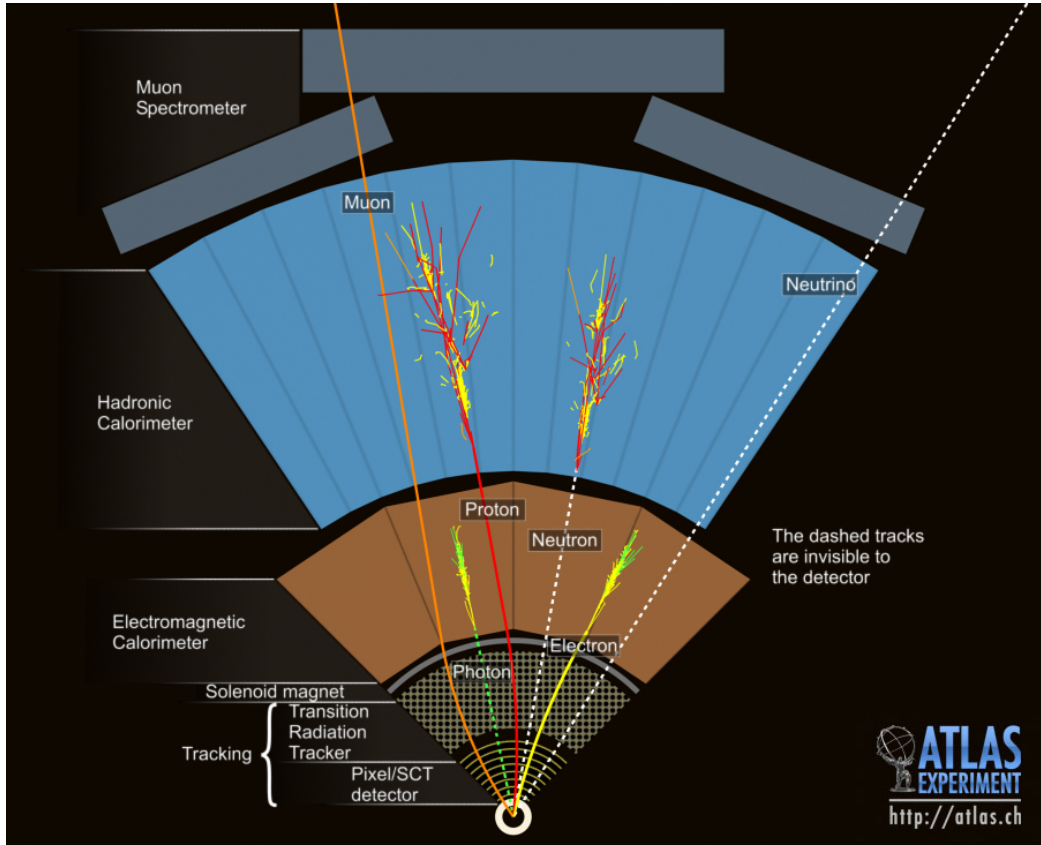


Figure 2.3: Event in the transverse plane, a computer generated image of the ATLAS detector [15].

The next two layers are the two calorimeters that measure energies of specific type of particles. The particles travel through the detectors and lose their energy via interaction with its layers leaving energy deposits as they move through the material. The first one is the high-granularity Electromagnetic Calorimeter (EmCal) and it measures energies of electrons and photons. Coloured particles (gluons and quarks) form "jets" that travel further into Hadronic calorimeter (HCal) where they continue

their decays and also deposit their available energy. Both calorimeters are designed to provide good quality measurements of momentum and energy and cover the region $|\eta| < 4.9$.

The final detecting layer is the Muon spectrometer (MS), which tracks and measures charged particles, specifically muons. Muons do not interact with matter as strongly as electrons so they travel further without radiating much energy in the calorimeters. MS is immersed into a large toroidal magnet, that provides a magnetic field throughout the spectrometer and bends the trajectories of charged muons, which makes it possible to detect their charge and momentum. Any particles that are not covered by the described sub-detectors will escape undetected. These include neutrinos and, possibly, the LSP.

Triggers are used to select events by identifying signatures of various particles as well as using global event signatures, such as missing transverse energy [16]. A multilevel trigger system is used at ATLAS to select events that are of interest to further offline analysis. The first level is hardware-based and uses information from the calorimeters and muon spectrometer, the second and third levels are software-based and use information from all sub-detectors. Because the data at LHC is produced in staggering amounts employing efficient trigger systems is crucial to be able to extract information that is relevant for further analysis. At $\sqrt{s}=13$ TeV the spacing between bunches crossing is 25 ns and the collision rate is 40 MHz. This rate has to be reduced to $O(500$ Hz) to be able to keep data in permanent memory devices [17].

Ideally, a trigger should be able to retain maximum number of events that are interesting for physics analysis and reject as many background events as possible. In this regard the concept of trigger efficiency is very important, and this efficiency varies depending on the particular process that is being investigated. The overall goal is to reduce data from the raw amount to the size at which it can be stored permanently and at the same time keeping as many relevant events as possible.

CHAPTER III

Search for supersymmetry at the LHC

3.1 Introduction

Searches for various BSM theories including SUSY have been performed at LHC alongside searching for the Higgs and performing different SM analyses. Many SUSY searches were conducted targeting the production of squarks and gluinos. This was motivated by a larger theoretical cross-section and therefore higher probability of producing coloured superpartners [18]. Up to this moment no statistically significant excess over SM has been detected and exclusion limits were placed on masses of SUSY particles. Figure 3.1 shows the latest data on the masses that have been excluded for supersymmetric particles in various production scenarios. The lower limits on the masses of most squarks and gluinos in different searches significantly exceed 1 TeV [19]. As a consequence, if their production occurs, it is either extremely rare at present energies or requires higher energy of collision to leave an identifiable signature.

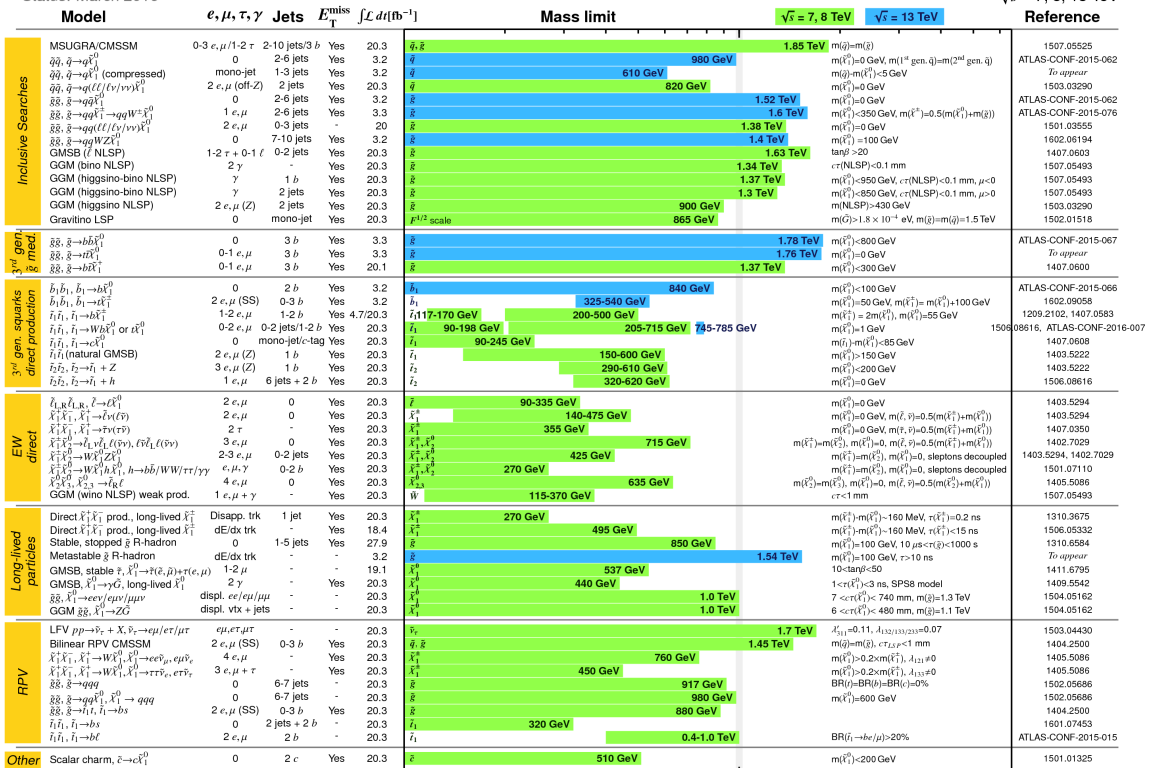
This thesis's research will focus on the electroweak production as one of the possible SUSY particle production scenario. Sleptons and gauginos are produced in electroweak production processes and are not affected by the strong force. They have smaller cross-sections compared to squarks and gluinos, so their theoretical production rate is smaller. However, if their masses are small compared to the strongly interacting sparticles, SUSY production will likely be dominated by electroweak production where sparticles have smaller mass and current energy might be enough to produce them in quantities that would allow their detection [20].

ATLAS SUSY Searches* - 95% CL Lower Limits

Status: March 2016

ATLAS Preliminary

$\sqrt{s} = 7, 8, 13 \text{ TeV}$



*Only a selection of the available mass limits on new states or phenomena is shown.

Figure 3.1: Exclusion limits of ATLAS searches for Supersymmetry. Squark and gluon masses are predominantly above the 1 TeV. [21]

So far searches in the electroweak region have been unable to find evidence of supersymmetric particles. Limits on their masses according to various decay scenarios have been obtained and can be seen in Fig 3.2.

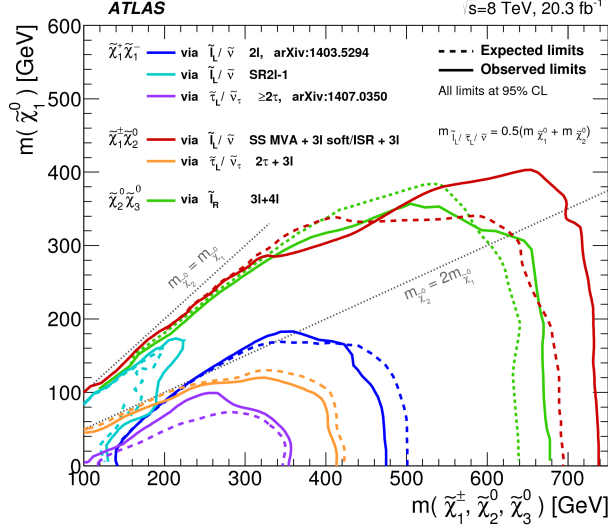


Figure 3.2: The 95% CL exclusion limits on $\chi_1^+ \chi_1^-$, $\chi_1^\pm \chi_2^0$ and $\chi_2^0 \chi_3^0$ production with $\tilde{\ell}$ -mediated decays, as a function of the χ_1^\pm , χ_2^0 and χ_3^0 masses [22].

These results are taken from [20] analysis performed at $\sqrt{s} = 8$ TeV and integrated luminosity of 20.3 fb^{-1} . The search was performed based on various scenarios of the MSSM, involving electroweak production of charginos and neutralinos. The turquoise and blue lines represent decay scenarios that are relevant for this paper as they show information on slepton-mediated decays of a chargino pair. In particular, the production of $\tilde{\chi}_1^+ \tilde{\chi}_1^-$ pair decaying through a slepton ($\tilde{\ell}$) with final states containing two opposite sign leptons will be considered (see Fig. 3.3).

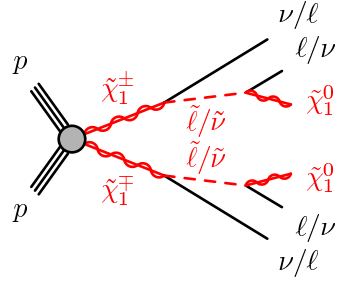


Figure 3.3: Electroweak chargino pair production in proton-proton collisions with intermediate slepton in the decay process.

The cross-section of this production process depends on the mass of the chargino

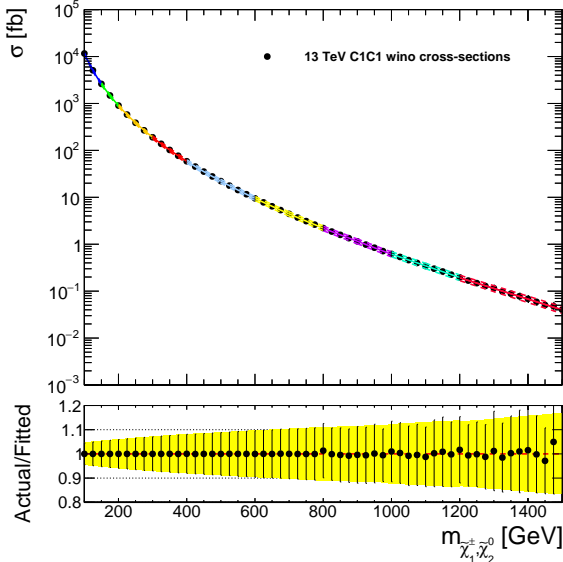


Figure 3.4: The distribution of cross-sections for slepton-mediated chargino decay [25].

- less heavy ones are more likely to be produced and therefore have a larger cross-sections. Fig. 3.4 shows the distribution of the theoretical cross sections depending on the mass of the chargino. The cross sections for this process were obtained from [23, 24].

In the nomenclature used at LHC and in this thesis, electrons and muons are called "light leptons". Taus are considered separately as they decay very promptly and therefore are very difficult to reconstruct. This thesis only focuses on final states containing electrons and muons and thus the designation "lepton" only refers to these particles.

3.2 General search methods

Detecting new physics events at LHC requires using computational and statistical methods that can deal with the type of information a particle accelerator produces. The data is initially collected using triggers corresponding to the type of events under analysis. Each event has a large number of physical characteristics such as momentum, energy, mass, multiplicities, etc. The numbers representing them are all stored in a data structure which then can be accessed, modified and analysed using software tools.

The cornerstone of all accelerator physics analyses is the correct estimation of background events. All background events represent physics that is already known

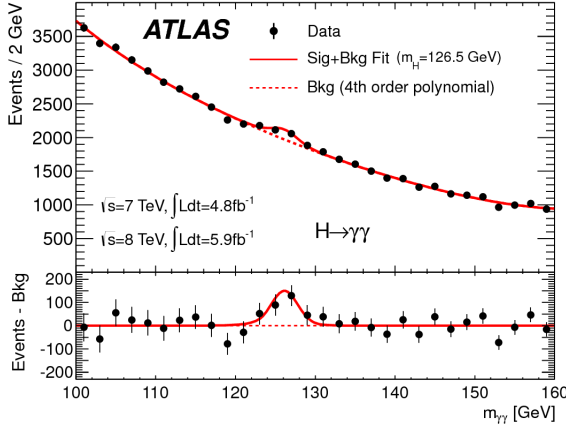


Figure 3.5: Invariant mass distribution of diphoton candidates for the combined $\sqrt{s} = 7$ TeV and $\sqrt{s} = 8$ TeV data samples. The mass of the Higgs corresponds to the peak at 126.5 GeV [1].

and that has some similar or identical features with the processes we wish to study. For instance, this thesis focusses on the reactions that have precisely two oppositely charged leptons in their final states. A number of processes well described by the standard model share this characteristic and therefore will form the background.

The task of correctly identifying background is therefore crucial in the process of searches for new physics events. Monte Carlo (MC) simulations are used to generate background events distribution samples according to a probability density function of a particular process. In this thesis MC simulated data samples are used to model SM background events along with SUSY signal events. All the samples include events that can result in dileptonic decays.

The data is then overlaid on the simulated background to see whether there is a disagreement between data and background. If there is a significantly large excess of data over background it can lead to new discoveries such as existence of a new particle. The presence of a new particle can reveal itself in a number of ways. The easiest case to detect is finding an abnormality in mass distribution, as was the case with the discovery of the Higgs. The narrow peak over a smooth line in mass distribution of diphoton events constituted a significant excess over SM predictions and was in agreement with theoretical predictions [1].

Unfortunately, this method does not work well for SUSY particles and other techniques have to be used. Standard search techniques involve defining **signal regions** in data distributions that are sensitive to possible SUSY signals and looking whether there is a significant excess over SM background predictions in these regions. This also includes looking for abnormal tails in distributions of different variables that

are not in agreement with SM predictions. These variables will be discussed in the subsection 3.4.1. Signal regions are usually determined using cut-and-count approach that will be discussed in the subsection 3.5.

3.3 Overview of background processes

In order to distinguish new physics events from SM events it is necessary to be able to suppress all SM events that have the same final state. Within the scope of this thesis that includes events that have precisely two leptons with opposite charge. The processes described in this section constitute MC simulated background that was used in the search for signal regions.

The Z +jets background comes from the production of jets of particles in association with a Z boson, which then decays into two leptons. $t\bar{t}$ pair creation is a common process in pp collisions and is one of the dominant processes in dilepton decays. The quark-antiquark pair decays via $W^+bW^-\bar{b}$ intermediate state into three different final states with no leptons, one lepton, and two leptons (here leptons include the tau). The latter decay cascade is $t\bar{t} \rightarrow W^+bW^-\bar{b} \rightarrow \ell\nu\ell\nu b\bar{b}$. Final states that include electrons and muons constitute around 5% of the entire $t\bar{t}$ production [26]. Thus, the $t\bar{t}$ production is one of the main background processes in searches for BSM events in various channels, not only those involving two-lepton final states.

Diboson production channel is dominated by the production of WW pair with subsequent decay into two lepton/neutrino pairs. Contributions also come from ZV channel, where $V = W$ or Z . Other sources of dilepton final states are W +jets and single-top quark production processes. Both of them have a decay channel with final states containing a lepton and a neutrino, however their overall contribution to the background is small compared to diboson, $t\bar{t}$, and Z +jets. All the MC background predictions used in this thesis belong to one of the categories described in this section.

3.4 Event selection and b -tagging

Event reconstruction is the process of turning raw data into manageable format that includes quantities needed in physics analysis. An event has to pass certain identification criteria to be chosen for reconstruction. Correct identification of different physics objects at LHC includes a large number of dedicated algorithms which are not presented in this thesis, but are available elsewhere [27]. However, in this section a very general outline of the selection procedure for reactions that result in two leptonic

decays will be given. All "signal" objects have to pass a set of criteria to obtain a high quality sample with minimum possible contamination.

Signal electrons are required to have $|\eta| < 2.47$ and transverse momentum $p_T > 10$ GeV. These are inferred from the calibrated energy deposits in the EmCal and must have a matching ID track. Signal muons are reconstructed using information from MS and ID tracks and are required to have $|\eta| < 2.5$ and $p_T > 10$ GeV. Jets are reconstructed using information from calorimeters and are divided into "central" and "forward" categories. Central jets must have $|\eta| < 2.4$ and $p_T > 20$ GeV. Forward jets are those with $2.4 < |\eta| < 4.5$ and $p_T > 30$ GeV.

One of the common techniques used in LHC analyses is the identification of central jets that have b -hadrons (hadrons containing bottom quark/s). These jets are referred to as b -tagged and are identified using multivariate techniques based on machine learning instruments such as artificial neural networks and boosted decision trees [28]. The efficiency of b -tagging has been significantly improved in run-II due to the addition of the Insertable B-Layer in the ID. b -tagging is an extremely useful technique because some important heavy particles such as top quark and the Higgs decay into bottom quarks.

3.4.1 Event variables used in the analysis

A set of discriminating variables associated with searches for evidence of SUSY is presented here. Topological and kinematic variables as well as quantities derived from them will be investigated.

\mathbf{p}_T^X The transverse momentum of an object X .

$\Delta\phi(\mathbf{X}, \mathbf{Y})$ The separation between two reconstructed objects X and Y , e.g. $\Delta\phi(E_T^{miss}, \ell)$.

E_T^{miss} The magnitude of the missing transverse momentum of the event. Missing transverse momentum is defined as the negative vector sum of the transverse momenta of all identified objects.

$E_T^{miss,rel}$ This value is defined as

$$E_T^{miss,rel} = \begin{cases} E_T^{miss} & \text{if } \Delta\phi(E_T^{miss}, \ell/j) \geq \pi/2, \\ E_T^{miss} \times \sin\Delta\phi(E_T^{miss}, \ell/j) & \text{if } \Delta\phi(E_T^{miss}, \ell/j) < \pi/2 \end{cases}$$

where $\Delta\phi(E_T^{miss}, \ell/j)$ is the azimuthal angle between the direction of $E_T^{miss,rel}$ and that of the nearest electron, muon, or central jet.

$\mathbf{p}_{T,\ell\ell}$ The transverse momentum of the two-lepton system.

$m_{\ell\ell}$ The invariant mass of the two leptons.

Another derived event variable is the so-called "stransverse mass" m_{T2} which was introduced as a way to infer information about undetected particles [29, 30]. Along with that it is also proved useful in suppressing backgrounds. It is used to bound the masses of a pair of supersymmetric particles each of them decaying into one visible and one invisible particle. It is a function of the momenta of two visible particles and the missing transverse momentum of an event. Its short mathematical description is as follows

$$m_{T2} = \min_{\mathbf{q}_T} \left[\max \left(m_T(\mathbf{p}_T^{\ell 1}, \mathbf{q}_T), m_T(\mathbf{p}_T^{\ell 2}, \mathbf{p}_T^{miss} - \mathbf{q}_T) \right) \right], \quad (3.1)$$

where $\mathbf{p}_T^{\ell 1}$ and $\mathbf{p}_T^{\ell 2}$ are the transverse momenta of the two leptons, and \mathbf{q}_T is a transverse vector that minimizes the larger of two transverse masses m_T which is defined as

$$m_T(\mathbf{p}_T, \mathbf{q}_T) = \sqrt{2(p_T q_T - \mathbf{p}_T \cdot \mathbf{q}_T)}. \quad (3.2)$$

3.5 Cut-and-count approach and test statistics

As was discussed previously a good signal region retains as many signal events as possible while at the same time cutting off background events. The way to suppress the background is to use successive cuts. The cuts are based on determining physical quantities that are able to discriminate between signal and background. The choice for a single cut is motivated both by theoretical considerations and the shapes of the MC signal and background distributions.

To optimize a cut or a set of cuts a metric that shows their discriminating power is needed. The numerical expression of how well a cut performs is given by a score function and its result will be referred to as "significance". The score function is constructed in the following way. The total number of events in a particular selection N , and it is the sum of S and B , which refer to the number of signal and background events respectively. And this gives

$$S = N - B \quad (3.3)$$

The uncertainty of S is then

$$\sigma^2(S) = \sigma^2(N) + \sigma^2(B) = N + \sigma^2(B) \quad (3.4)$$

N is a mean value of a Poisson process where uncertainty is $\sigma = \sqrt{\lambda}$, so squaring it back gives just N . $\sigma(B)$ is the uncertainty on the estimated average of B value. Because estimation of the background is done with large MC statistics the $\sigma(B)$ in this case can be treated as negligible. So what is left is

$$\frac{S}{\sigma(S)} = \frac{S}{\sqrt{N}} = \frac{S}{\sqrt{S+B}} \quad (3.5)$$

This determines the number of standard deviations away from 0 of the signal. Due to SUSY signals being very small compared to the background further simplification can be done, so that the above expression becomes

$$\frac{s}{\sigma(s)} \simeq \frac{S}{\sqrt{B}} \quad (3.6)$$

Here the important concept of p-value will be introduced.

Bibliography

- [1] G. Aad *et al.*, “Observation of a new particle in the search for the Standard Model Higgs boson with the ATLAS detector at the LHC,” *Phys. Lett.*, vol. B716, pp. 1–29, 2012.
- [2] S. Chatrchyan, V. Khachatryan, A. M. Sirunyan, A. Tumasyan, W. Adam, E. Aguilo, T. Bergauer, M. Dragicevic, J. Erö, C. Fabjan, *et al.*, “Observation of a new boson at a mass of 125 gev with the cms experiment at the lhc,” *Physics Letters B*, vol. 716, no. 1, pp. 30–61, 2012.
- [3] B. R. Martin, *Nuclear and particle physics: An introduction*. John Wiley & Sons, 2006.
- [4] S. L. Glashow, “Partial Symmetries of Weak Interactions,” *Nucl. Phys.*, vol. 22, pp. 579–588, 1961.
- [5] S. Weinberg, “A model of leptons,” *Physical review letters*, vol. 19, no. 21, p. 1264, 1967.
- [6] A. Salam and N. Svartholm, “Elementary particle theory,” *Almqvist and Wiksell, Stockholm*, p. 367, 1968.
- [7] F. Englert and R. Brout, “Broken symmetry and the mass of gauge vector mesons,” *Physical Review Letters*, vol. 13, no. 9, p. 321, 1964.
- [8] P. W. Higgs, “Broken symmetries and the masses of gauge bosons,” *Physical Review Letters*, vol. 13, no. 16, p. 508, 1964.
- [9] E. Gildener, “Gauge-symmetry hierarchies,” *Phys. Rev. D*, vol. 14, pp. 1667–1672, Sep 1976.
- [10] P. A. Ade, N. Aghanim, M. Alves, C. Armitage-Caplan, M. Arnaud, M. Ashdown, F. Atrio-Barandela, J. Aumont, H. Aussel, C. Baccigalupi, *et al.*, “Planck 2013 results. I. overview of products and scientific results,” *Astronomy & Astrophysics*, vol. 571, p. A1, 2014.
- [11] CMS , “Are there more particles left to find? supersymmetry: uniting the forces,” 2011. [Online; accessed May 18, 2016].

- [12] J. D. Lykken, “Introduction to supersymmetry,” in *Fields, strings and duality. Proceedings, Summer School, Theoretical Advanced Study Institute in Elementary Particle Physics, TASI’96, Boulder, USA, June 2-28, 1996*, pp. 85–153, 1996.
- [13] G. Aad, E. Abat, J. Abdallah, A. Abdelalim, A. Abdesselam, O. Abdinov, B. Abi, M. Abolins, H. Abramowicz, E. Acerbi, *et al.*, “The atlas experiment at the cern large hadron collider,” *Journal of Instrumentation*, vol. 3, no. 8, 2008.
- [14] G. Aad, B. Abbott, J. Abdallah, A. Abdelalim, A. Abdesselam, O. Abdinov, B. Abi, M. Abolins, H. Abramowicz, H. Abreu, *et al.*, “The atlas inner detector commissioning and calibration,” *The European Physical Journal C*, vol. 70, no. 3, pp. 787–821, 2010.
- [15] Pequenao, Joao, “Event cross section in a computer generated image of the atlas detector.,” 2008. [Online; accessed May 18, 2016].
- [16] G. Aad, B. Abbott, J. Abdallah, A. Abdelalim, A. Abdesselam, O. Abdinov, B. Abi, M. Abolins, H. Abramowicz, H. Abreu, *et al.*, “Performance of the atlas trigger system in 2010,” *The European Physical Journal C*, vol. 72, no. 1, pp. 1–61, 2012.
- [17] G. Barr, R. Devenish, R. Walczak, and T. Weidberg, *Particle Physics in the LHC Era*. Oxford University Press, 2015.
- [18] C. Borschensky, M. Krämer, A. Kulesza, M. Mangano, S. Padhi, T. Plehn, and X. Portell, “Squark and gluino production cross sections in pp collisions at $\sqrt{s}=13, 14, 33$ and 100 tev,” *The European Physical Journal C*, vol. 74, no. 12, pp. 1–12, 2014.
- [19] G. Aad, B. Abbott, J. Abdallah, O. Abdinov, R. Aben, M. Abolins, O. AbouZeid, H. Abramowicz, H. Abreu, R. Abreu, *et al.*, “Summary of the searches for squarks and gluinos using $\sqrt{s} = 8$ tev pp collisions with the atlas experiment at the lhc,” *Journal of High Energy Physics*, vol. 2015, no. 10, pp. 1–100, 2015.
- [20] G. Aad *et al.*, “Search for the electroweak production of supersymmetric particles in $\sqrt{s}=8$ TeV pp collisions with the ATLAS detector,” *Phys. Rev.*, vol. D93, no. 5, p. 052002, 2016.
- [21] ATLAS collaboration, “Mass reach of atlas searches for supersymmetry,” 2016.
- [22] G. Aad, B. Abbott, J. Abdallah, O. Abdinov, R. Aben, M. Abolins, O. AbouZeid, H. Abramowicz, H. Abreu, R. Abreu, *et al.*, “Search for the electroweak production of supersymmetric particles in $s=8$ tev p p collisions with the atlas detector,” *Physical review D*, vol. 93, no. 5, p. 052002, 2016.
- [23] B. Fuks, M. Klasen, D. R. Lamprea, and M. Rothering, “Gaugino production in proton-proton collisions at a center-of-mass energy of 8 TeV,” *JHEP*, vol. 10, p. 081, 2012.

- [24] B. Fuks, M. Klasen, D. R. Lamprea, and M. Rothering, “Precision predictions for electroweak superpartner production at hadron colliders with RESUMMINO,” *Eur. Phys. J. C*, vol. 73, p. 2480, 2013.
- [25] ATLAS collaboration, “13 tev c1c1 wino cross-section,” 2016.
- [26] W. Wagner, “Top-Antitop-Quark Production and Decay Properties at the Tevatron,” *Mod. Phys. Lett.*, vol. A25, pp. 1297–1314, 2010.
- [27] G. Aad *et al.*, “Search for supersymmetry at $\sqrt{s} = 13$ TeV in final states with jets and two same-sign leptons or three leptons with the ATLAS detector,” *Eur. Phys. J.*, vol. C76, no. 5, p. 259, 2016.
- [28] G. Aad *et al.*, “Performance of b -Jet Identification in the ATLAS Experiment,” *JINST*, vol. 11, no. 04, p. P04008, 2016.
- [29] C. G. Lester and D. J. Summers, “Measuring masses of semiinvisibly decaying particles pair produced at hadron colliders,” *Phys. Lett.*, vol. B463, pp. 99–103, 1999.
- [30] A. Barr, C. Lester, and P. Stephens, “ $m(T2)$: The Truth behind the glamour,” *J. Phys.*, vol. G29, pp. 2343–2363, 2003.